analytical chemistry

Article

pubs.acs.org/ac

Ehrlich Reaction Evoked Multiple Spectral Resonances and Gold Nanoparticle Hotspots for Raman Detection of Plant Hormone

Fangyuan Wang,[†] Xiaoling Gu,[†] Chunchen Zheng,[†] Fang Dong,[†] Liying Zhang,[†] Yueqing Cai,[†] Zhengyi You,[†] Junhui You,[†] Shuhu Du,*[,†] and Zhongping Zhang[‡,§]

[†]School of Pharmacy, Nanjing Medical University, Nanjing, Jiangsu 211166, China

[‡]School of Chemistry and Chemical Engineering, Anhui University, Hefei, Anhui 230601, China

[§]State Key Laboratory of Transducer Technology, Chinese Academy of Sciences, Hefei, Anhui 230031, China

S *Supporting Information*

ABSTRACT: Surface-enhanced Raman scattering (SERS) by use of noble metal nanoparticles has become a powerful tool to determine a low-concentration target by unique spectral fingerprints, but it is still limited to the Raman-inactive and nonresonant biomolecules such as amine acids, proteins, and hormones. Here, we report an Ehrlich reaction based derivative strategy in combination with gold nanoparticles (Au NPs) hotspots for the selective detection of indole-like plant hormones by SERS spectroscopy. Ehrlich reaction of *p*-(dimethylamino)benzaldehyde (PDAB) with the indole ring chemically transformed plant hormone indole-3-butyric acid (IBA) into a Raman-active and resonant derivative with an extended π-conjugated system in the form of a cation, which produced a new absorption band at 626 nm. On the other hand, cationic IBA−PDAB highly evoked the aggregation of Au NPs with negative citrate ligands to form the effective Raman hotspots and gave rise to the new absorption ranging from 600 to 800 nm. Significantly, the spectral overlap among IBA−PDAB, aggregated Au NPs, and the exciting laser initiated the multiple optical resonances to generate the ultrahigh Raman scattering with a sensitive limit of 2.0 nM IBA. The IBA in the whole sprouts and various parts of pea, mungbean, soybean, and black bean has been identified and quantified. The reported method opens a novel avenue for the SERS detection of Raman-inactive analyte by a proper derivation.

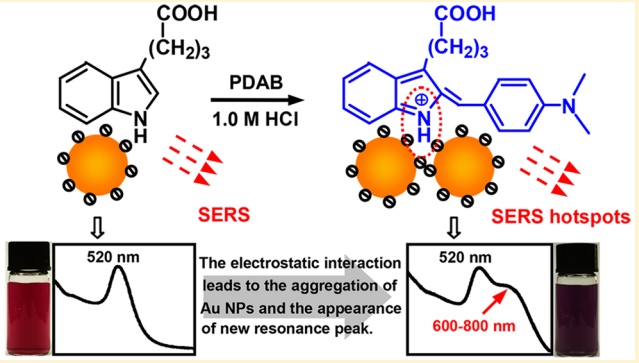

Plant hormones play a critical role in regulating the growth, differentiation, and development of plants as well as their responses to both biotic and abiotic stresses.[1] Such physiological functions are not only closely related with the endogenous concentration of plant hormones, but also depend on their existing parts or organs in plant systems.[2−4] Therefore, the determination of hormone levels in the whole plant is basically important for deeply understanding the molecular mechanism of plant hormones. To date, many techniques have been developed for the quantification of plant hormones, including gas chromatography/mass spectrometry (GC/MS),[5] high-performance liquid chromatography/mass spectrometry (HPLC/MS),[6] enzyme-linked immunosorbent assay (ELISA),[7] flow injection fluorimetry,[8] capillary electrophoresis−chemiluminescence,[9] and visual colorimetry.[10] On one hand these previously reported methods are difficult to detect the ultralow-level plant hormones due to their less sensitivity and selectivity, and on the other hand they are usually time-consuming and need tedious sample pretreatments and enrichments. Thus, there is a great demand for developing a sensitive, fast, and simple assay of plant hormones.

Recently, surface-enhanced Raman scattering (SERS) has been greatly developed as a powerful tool for the identification and detection of chemo/bio species by the use of noble metal nanoparticles,[11] which endows Raman spectroscopy with the multiple advantages of high sensitivity, unique spectroscopic fingerprints, and nondestructive data acquisition.[12,13] In principle, the electromagnetic (EM) field experienced by an interest molecule at the rough metal surface can greatly amplify the Raman scattering signals of the molecule.[14−16] Further, the metal nanoparticle aggregates or nanostructural junctions can maximize the EM field to form "hotspots" that obtain the ultrahigh Raman scattering comparable to the rough metal surfaces.[17,18] By the employment of the hotspots' enhancement, electronically resonated dyes can exhibit an enhancement factor as high as 10^{11}−10^{14}, and even the single-molecular signals.[19] Different from the resonant dyes, however, most of interest molecules are Raman-inactive even if enhanced due to a much smaller scattering cross section, limiting the applications of SERS in many fields.[20]

Received: April 5, 2017
Accepted: July 26, 2017
Published: July 26, 2017

DOI: 10.1021/acs.analchem.7b01267
Anal. Chem. 2017, 89, 8836−8843

It is well-known that the visible chromophores of resonant dyes may provide 2−3 orders of magnitude of additional enhancement relative to surface enhancement alone.[21,22] Recent investigations have revealed that bianalyte techniques by adding or modifying a chromophore can enhance the Raman signals of preresonant molecules.[23,24] The chromophore coupled to the localized surface plasmon of an active nanostructure leads to spectral resonance and surface enhancement.[25−27] These imply that the ultrastrong Raman enhancement of nonresonant molecules is possible by multiple resonance techniques.

In the present work, Ehrlich reaction was used to chemically transform the indole-like hormone indole-3-butyric acid (IBA) into a Raman-active resonant molecule and the ultrasensitive detection of IBA was achieved by the SERS approach through the employment of gold nanoparticles (Au NPs). IBA is the second discovered plant hormone that plays a key role in promoting the root development of plants.[9] Its concentration is at the nanogram scale per gram of plants, and thus the usual analytical methods are difficult to achieve its accurate quantification. Here, the transformed cationic derivative of IBA has a visible absorption band and can spontaneously induce the aggregation of Au NPs to generate the Raman hotspots. Interestingly, the absorption spectrum of the cationic derivative displays a large overlap with that of aggregated Au NPs. When the suitable exciting wavelength is chosen, the multiple spectral resonances among target molecule, Au NPs, and exciting light extremely enhance the SERS signals. Together with "hotspots"-initiated enhancement, the ultrastrong Raman scattering signals provide an ultrasensitive detection of IBA for the determination and quantification of IBA in the whole sprouts and various parts of mungbean, black bean, soybean, and pea.

EXPERIMENTAL SECTION

Chemicals and Materials. Sodium citrate ($Na_3C_6H_5O_7 \cdot 2H_2O$, 99.8%), chloroauric acid ($HAuCl_4 \cdot 4H_2O$, 99.9%), and hydrochloric acid (HCl, 36.5%) were purchased from Sinopharm Chemical Reagent Co., Ltd. (Shanghai, China). *p*-(Dimethylamino)benzaldehyde (PDAB, 99.5%), indole-3-butyric acid (IBA, 99.5%), indole-3-acetic acid (IAA, 99.5%), naphthylacetic acid (NAA, 96.5%), abscisic acid (ABA, 95.5%), gibberellin (GA, 95.5%), jasmonic acid (JA, 95.5%), and salicylic acid (SA, 95.5%) were supplied by Aladdin reagent Co., Ltd. (Shanghai, China). These reagents were of analytical grade and used as received without further treatment. Methanol, acetonitrile, and acetic acid were of HPLC grade and purchased from Sinopharm Chemical Reagent Co., Ltd. (Shanghai, China). Ultrapure water (18.2 MΩ cm) was produced using a Millipore water purification system (Milford, MA, U.S.A.).

Preparation of Au NPs. The 30 nm sized Au NPs were prepared by the reduction of $HAuCl_4$ with sodium citrate as described in our previous work.[28] Briefly, 2.5 mL of 0.1 M chloroauric acid and 100 mL of ultrapure water were mixed in a three-necked flask and then heated to boiling under magnetic stirring. After quickly injecting 1.5 mL of trisodium citrate (1%, w/w), the mixture solution was kept refluxing for 30 min until the solution color became wine red. Au NPs colloid was finally obtained after gradually cooling to room temperature. For comparison, larger Au NPs (60 nm) and smaller Au NPs (15 nm) were also synthesized using the same method, but varying the amount of 1% trisodium citrate (0.4 and 4.0 mL, respectively). UV−vis absorption spectra, transmission electron microscopic (TEM) images, and dynamic light scatterings (DLS) of Au NPs with different sizes are shown in Figure S-1. The concentrations of Au NPs with the sizes of 15, 30, and 60 nm are ∼0.41, ∼0.24, and ∼0.06 nM, respectively, which are calculated by Beer's law and the extinction coefficients (ε) (15, 30, and 60 nm Au NPs are 2.0×10^8, 3.0×10^9, and 1.7×10^{10} M^{-1} cm^{-1}, respectively[29]). Before use, the concentrations of three Au NPs were adjusted to 0.24 nM.

Preparation and Purification of IBA−PDAB. IBA (30.5 mg) and PDAB (89.5 mg) were dissolved in 60 mL of 50% methanol solution containing 1.0 M HCl, and stirred at a 30 °C water bath for 2 h. Then, the methanol solvent and HCl were removed under reduced pressure. The resulting precipitate was dissolved in 10 mL of methanol, and the pH value of the mixture solution was measured to be about 5. After purification through HPLC, the reaction product IBA−PDAB was obtained as a blue solid (yield: ∼46.7%). MS *m*/*z* 335.2 $[M + H]^+$ (calcd for $C_{21}H_{23}N_2O_2$ 335.2). See the detailed results in Figure S-2.

Preparation and Pretreatment of Real Samples. Mungbean, black bean, pea, and soybean were purchased from the local supermarket in Nanjing, China. The four beans were soaked in tap water for 12 h, and then germinated in a tray covered with a plastic membrane under a suitable temperature and humidity. The water was refreshed per day throughout the growth period. The whole sprouts and various parts of pea, mungbean, soybean, and black bean were collected. About 2.0 g of sample was soaked in 15 mL of methanol/water (80:20 v/v), followed by ultrasonic extraction for 15 min. The supernatant containing IBA was stored in refrigerator at 4 °C for further use.

SERS Detection of IBA in Bean Sprouts. Typically, 0.2 mL of extract solution of mungbean sprout was added into 0.2 mL of 400 μM PDAB, and then reacted in the presence of 1.0 M HCl at a 30 °C water bath for 2 h. After 10 μL of reaction mixture was added into 90 μL of Au NPs colloid, the final mixture was sucked into a capillary glass tube and fixed onto a glass slide. The SERS spectra were recorded using the 633 nm laser with 6 mW power and 10× objective. The collecting time was 4 s with five rounds of accumulations, and the pinhole aperture was 25 μm. The other samples including the whole sprouts of black bean, pea, and soybean as well as the various parts of mungbean seedlings were also done by the same method.

Characterization and Instruments. The prepared Au NPs were characterized by a JEM-1010 transmission electron microscopy (TEM) instrument (Tokyo, Japan). The hydrodynamic sizes of NPs were determined using a Malvern Zetasizer Nano-ZS90 particle size analyzer (Malvern, U.K.). UV−vis absorption spectra were obtained by a UV-2501 spectrometer (Tokyo, Japan). Raman measurements were conducted with a Thermo Fisher DXR Raman microscope equipped with a CCD detector in backscattered configuration using a 10× objective (Madison, WI, U.S.A.). HPLC chromatograms were recorded with a Shimadzu HPLC system equipped with an LC-20AT pump, SPD-M20A detector, and CTO-20A column oven (Tokyo, Japan). MS was performed on an Agilent 6410B triple quad LC−ESI-MS/MS (Palo Alto, CA, U.S.A.).

RESULTS AND DISCUSSION

Ehrlich Reaction between IBA and PDAB. The typical Ehrlich reaction between *p*-(dimethylamino)benzaldehyde (PDAB) and an indole ring can produce a water-soluble colored cationic complex under acidic medium.[30,31] PDAB

DOI: 10.1021/acs.analchem.7b01267
Anal. Chem. 2017, 89, 8836−8843

molecule is first protonated at the carbonyl oxygen atom by hydrogen ion, and thus the carbonyl carbon atom is positively charged. Then, the protonated PDAB can initiate an electrophilic substitution reaction with the indole ring, followed by the elimination of a water molecule to form the final product (Figure S-3). Figure 1A shows that the similar reaction occurs

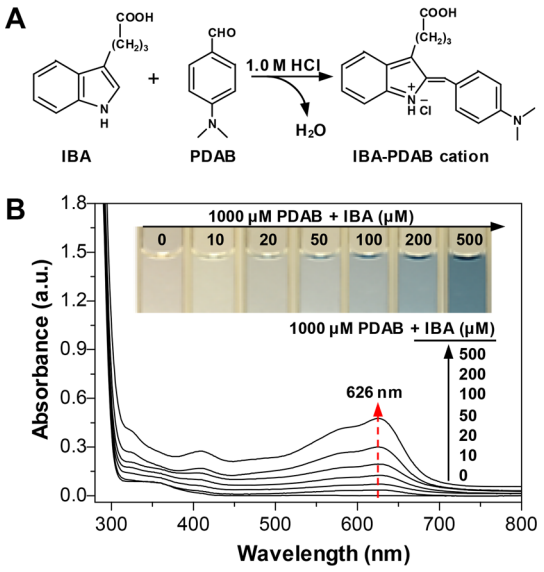

Figure 1. (A) Scheme for the reaction between IBA and PDAB in the presence of 1.0 M HCl. (B) UV−vis absorption spectral responses of PDAB solution (a fixed 1000 μM) with the addition of IBA (ranging from 0 to 500 μM) (inset images show the corresponding color changes from colorless into sky blue).

between IBA and PDAB in the presence of 1.0 M HCl. Ehrlich reaction chemically linked the indole ring with an aromatic ring by a double bond to produce a cationic derivative, which extended the π-conjugated system and formed a coupled chromophore. As shown in Figure 1B, a new visible absorption band appeared at ~626 nm and became stronger and stronger with the addition of IBA into PDAB solution. Meanwhile, the color of the reaction mixture changed from colorless to sky blue, as shown in the inset of Figure 1B. After purification, the resultant IBA−PDAB was characterized by MS (Figure S-2). These above observations clearly demonstrate that IBA can react with PDAB to form IBA−PDAB chromophore.

Interaction between IBA−PDAB and Au NPs. The 30 nm Au NPs were synthesized by the reduction of $HAuCl_4$ with sodium citrate in aqueous solution. The resulting citrate-capped Au NPs were negatively charged, and the aggregation will quickly occur upon the addition of IBA−PDAB cation into the Au NPs due to electrostatic interaction. With the increase of IBA−PDAB cation concentration from 0 to 100 μM, UV−vis spectra show a gradual decrease of original absorbance of Au NPs at 520 nm and appearance of a new absorption band ranging from 600 to 800 nm, indicating the occurrence of Au NPs aggregation (Figure 2A). At the same time, the addition of IBA−PDAB cation into the Au NPs colloid led to the color change from wine red, to purple, to final blue (the inset of Figure 2A). The aggregation of Au NPs was further confirmed by TEM observations: monodisperse Au NPs in the absence of IBA−PDAB cation (Figure 2B) and significant aggregation of Au NPs in the presence of 10 μM IBA−PDAB cation (Figure

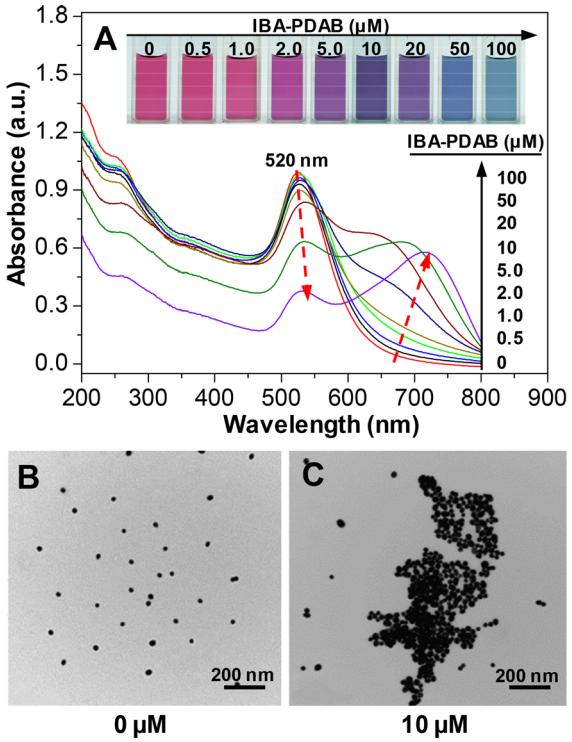

Figure 2. (A) Evolution of UV−vis absorption of Au NPs with the increase of IBA−PDAB cation concentration from 0 to 100 μM (inset images show the corresponding color changes from wine red to blue). (B and C) TEM images of Au NPs before and after the addition of 10 μM IBA−PDAB cation, respectively.

2C). More details on the characterizations of Au NPs aggregation are shown in Figures S-4 and S-5.

Moreover, similar experiments were also performed by the addition of pure PDAB, IBA, and the mixture of unreacted PDAB and IBA into Au NPs, respectively. However, Au NPs still remained intact without undergoing any aggregation by UV−vis spectral analysis (Figure S-6), which implied that the residual PDAB and IBA in the reaction system could not induce the aggregation of Au NPs.

Raman Enhancement Mechanism. Figure 3A illustrates the IBA−PDAB cation-evoked multiple spectral resonances Raman enhancement mechanism for detection of IBA using the Au NPs sensor. Due to the countercharged interaction, the aggregation of Au NPs occurs upon the direct exposure to IBA−PDAB cation, leading to the generation of Raman hotspots and the strong SERS readouts. When IBA was added into Au NPs, the aggregation does not occur and Raman signals almost cannot be detected. Different from the IBA molecule, however, IBA−PDAB cation has an electronic resonant state with a visible chromophore, which exhibits a visible absorbance centered at 626 nm (the blue line in Figure 3B). When the 633 nm laser is used to record the Raman spectrum, the blue chromophore can absorb the light and bring about electronic resonance to enhance the Raman signals of IBA−PDAB cation. Meanwhile, the spectral overlap between the chromophore absorbance and the surface plasmon of Au NPs aggregations (600−800 nm, purple line in Figure 3B) may result in the surface resonance enhancement. Together with the hotspots' effect, the multiple optical resonances will significantly enhance the Raman scattering signals of IBA−PDAB cation (Figure 3A).

DOI: 10.1021/acs.analchem.7b01267
Anal. Chem. 2017, 89, 8836−8843

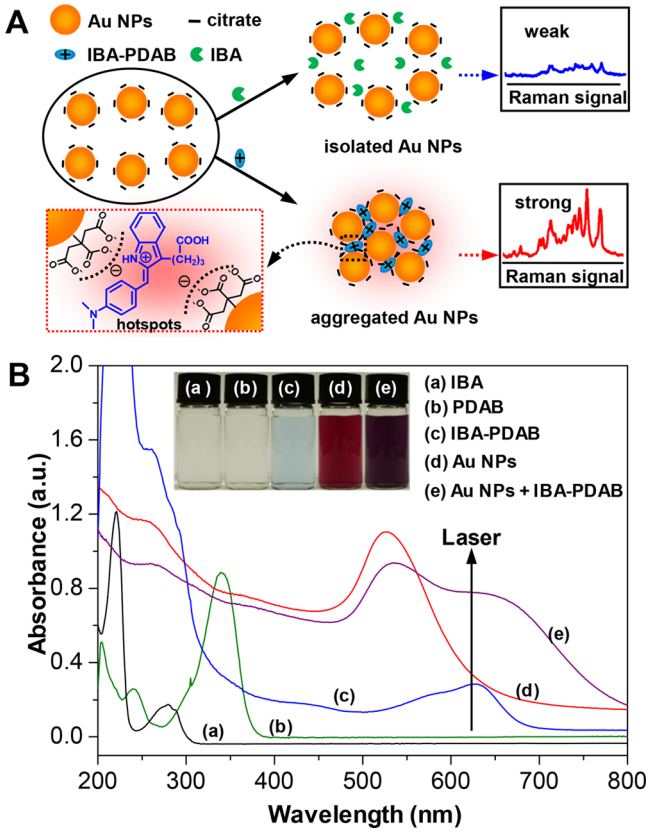

Figure 3. (A) Schematic illustration for the electrostatic interaction of IBA–PDAB cation with negatively charged Au NPs and the formation of Raman hotspots. (B) UV–vis absorption spectra of (a) 20 μM IBA, (b) 20 μM PDAB, (c) 20 μM IBA–PDAB cation, (d) Au NPs colloid, and (e) the mixture of IBA–PDAB cation and Au NPs colloid (inset are the corresponding color images).

To better understand the enhancement mechanism, we measured the Raman signals of pure IBA and PDAB in Au NPs colloid, and the SERS signals were still very weak even at the high concentration of 1000 μM (Figure S-7). However, the Raman signal of the 1600 cm^{-1} peak strengthened continuously with the addition of PDAB into IBA solution in the presence of 1.0 M HCl, and then kept unchanged at 2000 μM PDAB (Figure S-8). The assignments of all peaks from IBA–PDAB cation are listed in Table S-1. The enhancement factor calculated from the spectra before and after the addition of PDAB is about 76 (see the detailed procedure in Figure S-8). It has been demonstrated that the mentioned mechanisms can greatly enhance the SERS signals of IBA–PDAB cation by the derivation of IBA with PDAB.

It should be noted that the enhancement effect also depended on the size of Au NPs (Figure S-9). When the size of NPs was smaller than 30 nm, the Raman enhancement effect increased significantly with the size of Au NPs, in which the Raman intensity at 1600 cm^{-1} for 30 nm Au NPs was about 40-fold stronger than that of 15 nm Au NPs. The further increase of Au NPs size resulted in the decrease of enhancement effect (the Raman intensity at 1600 cm^{-1} for 60 nm Au NPs decreased about 50%), which was attributed to more instability of Au NPs with larger size.[32,33] Therefore, 30 nm Au NPs exhibited a much higher Raman enhancement effect on IBA–PDAB cation than 15 and 60 nm Au NPs, and can be used for the detection of IBA in all the following experiments.

Reactive Selectivity of PDAB with Indole-like Plant Hormones. Indole-3-acetic acid (IAA) is the plant hormone most similar to IBA in chemical structure (Figure 4A), and thus

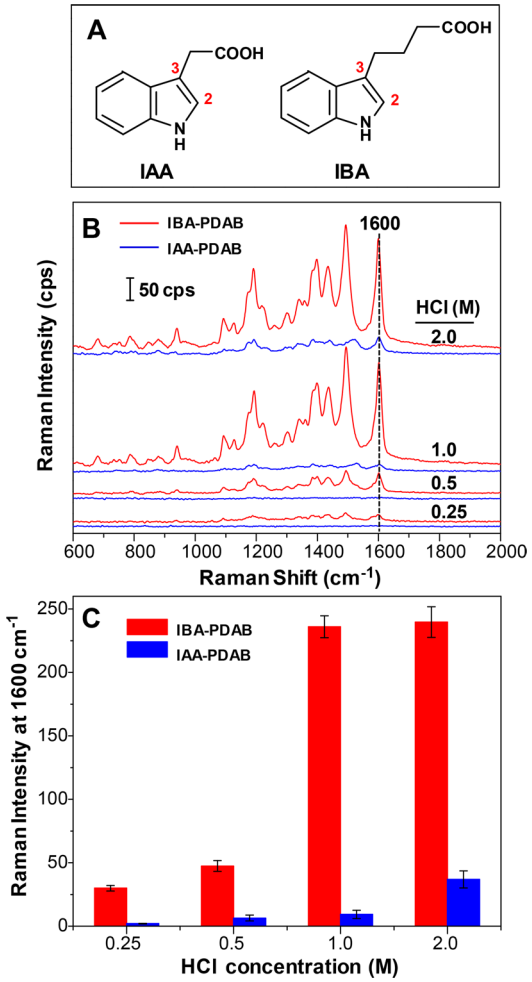

Figure 4. (A) Chemical structures of IAA and IBA. (B) SERS spectra of reaction products IBA–PDAB (red) and IAA–PDAB (blue) in Au NPs colloid at 0.25, 0.5, 1.0, and 2.0 M HCl (the used concentrations of IBA and IAA are all 0.2 μM). (C) Variations of corresponding reaction product Raman intensity at 1600 cm^{-1} with the increase of HCl concentration.

may exhibit the reactivity with PDAB. In the indole-ring structure, however, the electron-withdrawing group at the C-3 position can significantly decrease the electron density of the indole ring, weakening the nucleophilicity of the C-2 position.[30,34] Due to the strong electron-withdrawing effect of the acetoxy group of IAA at the C-3 position (Figure 4A), PDAB should have stronger reactivity with IBA than with IAA, which was investigated by the SERS spectroscopy. We monitored the reaction products IBA–PDAB and IAA–PDAB by the addition of IBA and IAA into PDAB solution at different HCl concentrations using the SERS spectra in Au NPs colloid (Figure 4B). While the Raman signals of IAA–PDAB at 0.25, 0.5, 1.0, and 2.0 M HCl could not be detected or were rather weak, the Raman signals of IBA–PDAB became stronger with the increase of HCl concentration. Moreover, the reaction sensitivity was accurately estimated by monitoring the intensity of the 1600 cm^{-1} Raman peak (Figure 4C). The Raman intensity of IBA–PDAB increased and reached the

DOI: 10.1021/acs.analchem.7b01267
Anal. Chem. 2017, 89, 8836–8843

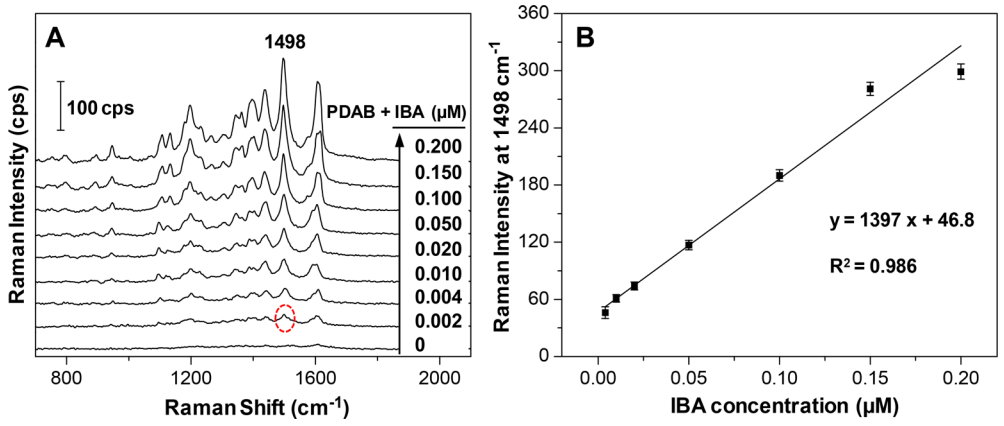

Figure 5. (A) SERS spectra of the reaction product IBA−PDAB with increase of IBA concentration in Au NPs colloid. (B) The linear correlation of Raman intensity at 1498 cm^{-1} with the IBA concentration from 0.004 to 0.20 μM.

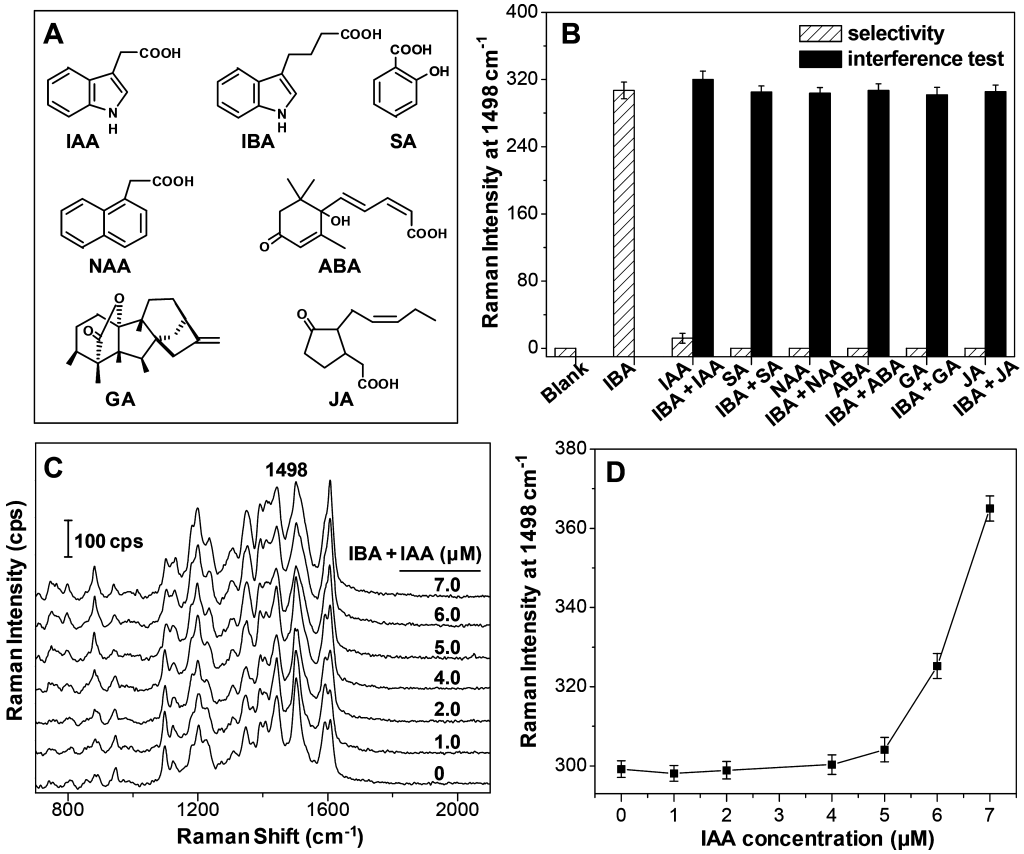

Figure 6. (A) Chemical structures of plant hormones: IAA, IBA, SA, NAA, ABA, GA, and JA. (B) Selectivity (striped columns) and interference test (black columns). The selectivity data were obtained using IBA (0.2 μM) and other plant hormones (5.0 μM). The anti-interference tests were performed by the addition of IBA (0.2 μM) containing an excess of interfering plant hormones (5.0 μM) into PDAB solution. (C) SERS spectra of the reaction solution of PDAB and IBA (0.2 μM) containing different concentrations of IAA (0, 1.0, 2.0, 4.0, 5.0, 6.0, and 7.0 μM) in Au NPs colloid. (D) Evolution of corresponding reaction product Raman intensity at 1498 cm^{-1}.

maximum at 1.0 M HCl, which was about 27-fold stronger than that of IAA−PDAB. When HCl concentration was up to 2.0 M, the Raman intensity of IAA−PDAB became obviously stronger, suggesting more production of IAA−PDAB cation (see the MS in Figure S-10). These results confirm that PDAB can selectively react with IBA over IAA in the presence of 1.0 M HCl to form IBA−PDAB cation. Thus, all tests in this work were performed at 1.0 M HCl.

Subsequently, we examined PDAB concentration and the time-dependent process to ensure reaction completion. The Raman signal at 1600 cm^{-1} of IBA−PDAB reached the maximum and kept unchanged at 400 μM PDAB, but only a feeble signal was observed in the case of IAA (Figures S-11 and S-12). The SERS spectra and the kinetic curves of IBA−PDAB and IAA−PDAB are shown in Figure S-13. With prolonging reaction time, the Raman signal at 1600 cm^{-1} was gradually enhanced and kept stable at 2 h in the two reaction systems, indicating the reactions were completed at this moment. Therefore, 1.0 M HCl, 400 μM PDAB, and reaction for 2 h

DOI: 10.1021/acs.analchem.7b01267
Anal. Chem. 2017, 89, 8836−8843

were employed as the optimized conditions throughout the following work.

Furthermore, we investigated the influence of HCl and IBA−PDAB cation on Au NPs by UV−vis absorption spectra and SERS spectroscopy (Figure S-14). With the addition of HCl, the absorption band of Au NPs at 520 nm only exhibited a slight decrease, and the Raman signals could not be detected at all. Upon the addition of IBA−PDAB cation, however, the absorbance at 520 nm decreased drastically, and the very strong Raman signals were obviously observed. The SERS spectra of IBA−PDAB cation changing from 0.02 to 4.0 μM in the Au NPs colloid were collected in the presence and absence of HCl (Figure S-15A), and their Raman intensities at 1600 cm^{-1} were nearly identical (Figure S-15B). These results suggest that IBA−PDAB cation is the main substance to cause aggregation of Au NPs and SERS enhancement, and HCl does not affect IBA detection.

Sensitivity and Selectivity for Detection of IBA. Figure 5A shows the SERS spectra of reaction product IBA−PDAB in Au NPs colloid with the addition of IBA into PDAB solution. The Raman signals were observed and became stronger and stronger with the increase of IBA concentration. The intensity of the strongest peak at 1498 cm^{-1} was used for the quantitative evaluation of IBA level and exhibited a good linear relationship with the concentration ranging from 0.004 to 0.20 μM (R^2 = 0.986) in Figure 5B. The detection limit was detected to be 0.002 μM (the red circle in Figure 5A), which was the lowest among these reported methods for IBA detection (Table S-2). These results suggest that low-concentration IBA can be quantitatively detected by the SERS approach.

To assess the reaction selectivity of PDAB to IBA over other plant hormones, including IAA, salicylic acid (SA), naphthylacetic acid (NAA), abscisic acid (ABA), gibberellin (GA), and jasmonic acid (JA) in Figure 6A, the SERS spectra were measured by the addition of other hormones into PDAB solution (Figure S-16). Herein, the separate Raman peak at 1498 cm^{-1} was selected as the evaluation indicator of the reaction selectivity. As shown in Figure 6B, the Raman intensity at 1498 cm^{-1} was remarkably enhanced upon the addition of IBA. Meanwhile, the Raman intensity seemed to be slightly enhanced after the addition of IAA. However, with the addition of SA, NAA, ABA, GA, and JA, there was not any Raman signal at 1498 cm^{-1} to be detected, which was identical to the blank PDAB, indicating an excellent selectivity of PDAB to IBA. Moreover, the anti-interference test of IBA detection was carried out in the coexistence of other plant hormones. With the addition of IBA (0.2 μM) containing other plant hormones (5.0 μM) into PDAB solution, the Raman intensity at 1498 cm^{-1} was unaffected by 25-fold excesses of the interfering plant hormones, but the slight enhancement could be observed in the case of IAA (Figure 6B). A main reason is that IAA at the higher concentration also reacted with PDAB.

Subsequently, the influence of IAA on IBA detection was further investigated by the addition of the mixture of IBA and IAA into PDAB solution, in which IBA concentration was fixed at 0.2 μM and IAA concentration from 0 to 7.0 μM. Figure 6C shows the SERS spectra of the final reaction mixtures in Au NPs colloid. When IAA concentration was lower than 5.0 μM, the Raman intensity at 1498 cm^{-1} kept unchanged and all the peaks were attributed to the reaction product IBA−PDAB. With the further increase of IBA concentration, the intensity of the 1498 cm^{-1} Raman peak was remarkably strengthened (Figure 6D). Although the higher concentration of IAA caused the increase of Raman intensity at 1498 cm^{-1}, the practical application of this strategy for detection of IBA in real samples is still feasible in view of the concentration of IAA in the plant tissues below 0.1 μM.[35,36]

Detection of IBA in Real Samples. To evaluate the usefulness of this method for determination of IBA in practical applications, the detection of endogenous IBA in real sample was first demonstrated herein by the derivative strategy coupled with Au NPs hotspots. Figure 7A illustrates the detection process of IBA in mungbean sprout. The sample only needed to be pretreated by ultrasonic extraction and centrifugation. The Raman signal at 1498 cm^{-1} of the blank sample can be clearly detected, as indicated with red circle in Figure 7B, and the concentration of endogenous IBA in the mungbean sprout was highly consistent with the HPLC result (Table S-3). When three known amounts of IBA were added into the mungbean sprout extracts, the recoveries of IBA ranged from 97.5% to

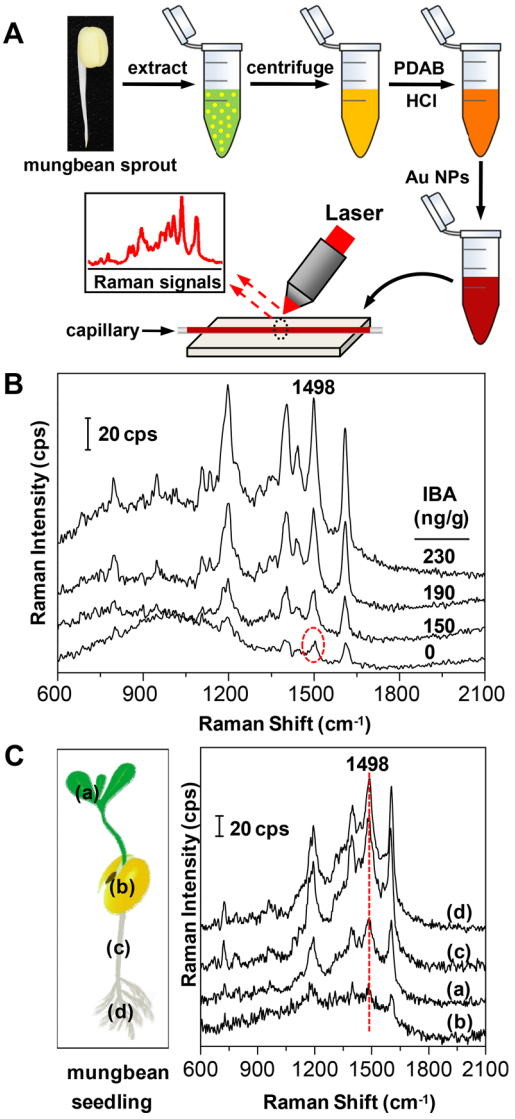

Figure 7. (A) Schematic drawing for the detection of IBA in the mungbean sprout by the SERS spectroscopy using Au NPs as Raman amplifier. (B) SERS spectra of the mungbean sprout extract spiked with IBA by the enhancement of Au NPs. (C) SERS spectra of the extract from the various parts of the mungbean seedling in Au NPs colloid: (a) leaf, (b) cotyledon, (c) hypocotyl, and (d) root tip.

DOI: 10.1021/acs.analchem.7b01267
Anal. Chem. 2017, 89, 8836−8843

101%. Afterward, similar results were also obtained from the other three kinds of bean sprouts (Figure S-17 and Table S-3). These confirm that the method has a high accuracy and reliability to satisfy the requirement of IBA detection in the bean sprouts.

Furthermore, the method can be employed to detect IBA in the various parts of mungbean seedlings, and the corresponding SERS fingerprints from the various parts are shown in Figure 7C. The Raman signal at 1498 cm^{-1} was very weak in the cotyledon, while the signal remained relatively strong in the hypocotyl and root tip, as indicated with the red line. The concentrations of endogenous IBA in the cotyledon, leaf, hypocotyl, and root tip were determined to be 14.8, 63.7, 154, and 181 ng/g, respectively. The above results indicate that IBA mainly exists in the growth activity sites, such as the root tip and the hypocotyl of the bean seedling, which was in agreement with the previous study.[37]

Additional Discussion on the Generalizability of This Technology. Generally, the Ehrlich reaction can transform a nonresonant molecule into a Raman-active molecule when a suitable reaction reagent is used, which adds a chromophore into an analyte to obtain strong Raman signals. There are a large number of indole-ring-containing molecules such as serotonin[38] and α-lactalbumin[39] in biological systems, ergometrine[40] in therapeutic drugs, and collagen[41] in cosmetics. Therefore, the reported approach by the combination of the Ehrlich reaction and SERS technique can potentially be applicable in the assays of proteins, drugs, and cosmetics through the reasonable modifications to the conditions of reaction and measurement. On the other hand, it should be noted that the efficiency of the Ehrlich reaction is closely related to the high nucleophilicity of the indole ring. That is to say, the indole-ring-containing molecules with different substituted groups exhibit distinctive reactivity, and thus the approach may provide a low detection sensitivity to some analytes.

CONCLUSIONS

In summary, we have successfully developed the Ehrlich reaction based derivative strategy in combination with Au NPs hotspots for the indirect detection of indole-like plant hormones by SERS spectroscopy. It has been demonstrated that PDAB can selectively react with IBA over IAA to form the effective IBA−PDAB cation at 1.0 M HCl, resulting in the spectral discrimination of IBA from IAA. Importantly, the spectral overlap among IBA−PDAB, aggregated Au NPs, and the exciting laser initiated the multiple optical resonances to obtain the ultrahigh sensitivity to IBA down to the nanomolar level, which enormously exceeds the previous literature results. Moreover, there is no serious matrix interference in detection of IBA from real samples. The as-developed strategy may have great potential for the dynamic assessment of plant hormones' content and the understanding of the molecular mechanism of plant hormones.

ASSOCIATED CONTENT

Supporting Information

The Supporting Information is available free of charge on the ACS Publications website at DOI: 10.1021/acs.analchem.7b01267.

UV−vis absorption spectra, TEM images, and DLS analysis of Au NPs, HPLC chromatograms, MS charts and SERS spectra of IBA−PDAB and IAA−PDAB, and SERS detection of IBA in different bean sprouts (PDF)

AUTHOR INFORMATION

Corresponding Author

*Phone: +86 25 86868476. Fax: +86 25 86868476. E-mail: shuhudu@njmu.edu.cn.

ORCID

Shuhu Du: 0000-0002-4819-0822

Notes

The authors declare no competing financial interest.

ACKNOWLEDGMENTS

This work is supported by the National Natural Science Foundation of China (Nos. 21275075 and 61605084).

REFERENCES

(1) Chen, J.; Du, X.; Zhao, H.; Zhou, X. *J. Plant Growth Regul.* **1996**, *15*, 173−177.
(2) Novák, O.; Hényková, E.; Sairanen, L.; Kowalczyk, M.; Pospíšil, T.; Ljung, K. *Plant J.* **2012**, *72*, 523−536.
(3) Ludwig-Müller, J.; Epstein, E. *Plant Growth Regul.* **1994**, *14*, 7−14.
(4) Ludwig-Müller, J. *Plant Growth Regul.* **2000**, *32*, 219−230.
(5) Ma, W.; Fu, S.; Hashi, Y.; Chen, Z. *J. Agric. Food Chem.* **2013**, *61*, 6288−6292.
(6) Sun, X.; Ouyang, Y.; Chu, J.; Yan, J.; Yu, Y.; Li, X.; Yang, J.; Yan, C. *J. Chromatogr. A* **2014**, *1338*, 67−76.
(7) Watanabe, E.; Tsuda, Y.; Watanabe, S.; Ito, S.; Hayashi, M.; Watanabe, T.; Yuasa, Y.; Nakazawa, H. *Anal. Chim. Acta* **2000**, *424*, 149−160.
(8) Calatayud, J. M.; de Ascencão, J. G.; Albert-García, J. R. *J. Fluoresc.* **2006**, *16*, 61−67.
(9) Yin, X.; Guo, J.; Wei, W. *J. Chromatogr. A* **2010**, *1217*, 1399−1406.
(10) Guo, J.; Xin, Y.; Yin, X. *J. Agric. Food Chem.* **2010**, *58*, 6556−6561.
(11) Mandal, M.; Jana, N.; Kundu, S.; Ghosh, S.; Panigrahi, M.; Pal, T. *J. Nanopart. Res.* **2004**, *6*, 53−61.
(12) Qian, X.; Nie, S. *Chem. Soc. Rev.* **2008**, *37*, 912−920.
(13) Abbas, A.; Brimer, A.; Slocik, J.; Tian, L.; Naik, R.; Singamaneni, S. *Anal. Chem.* **2013**, *85*, 3977−3983.
(14) Laurence, T. A.; Braun, G.; Talley, C.; Schwartzberg, A.; Moskovits, M.; Reich, N.; Huser, T. *J. Am. Chem. Soc.* **2009**, *131*, 162−169.
(15) Camden, J. P.; Dieringer, J. A.; Wang, Y.; Masiello, D. J.; Marks, L. D.; Schatz, G. C.; Van Duyne, R. P. *J. Am. Chem. Soc.* **2008**, *130*, 12616−12617.
(16) Krug, J. T.; Wang, G. D.; Emory, S. R.; Nie, S. *J. Am. Chem. Soc.* **1999**, *121*, 9208−9214.
(17) Haes, A. J.; Zou, S.; Zhao, J.; Schatz, G. C.; Van Duyne, R. P. *J. Am. Chem. Soc.* **2006**, *128*, 10905−10914.
(18) Nie, S.; Emory, S. R. *Science* **1997**, *275*, 1102−1106.
(19) Pieczonka, N. P. W.; Aroca, R. F. *Chem. Soc. Rev.* **2008**, *37*, 946−954.
(20) Maher, R. C.; Galloway, C. M.; Le Ru, E. C.; Cohen, L. F.; Etchegoin, P. G. *Chem. Soc. Rev.* **2008**, *37*, 965−979.
(21) Willets, K. A.; Van Duyne, R. P. *Annu. Rev. Phys. Chem.* **2007**, *58*, 267−297.
(22) Doering, W. E.; Nie, S. *Anal. Chem.* **2003**, *75*, 6171−6176.
(23) Qu, W.; Lu, L.; Lin, L.; Xu, A. *Nanoscale* **2012**, *4*, 7358−7361.
(24) Zhou, H.; Zhang, Z.; Jiang, C.; Guan, G.; Zhang, K.; Mei, Q.; Liu, R.; Wang, S. *Anal. Chem.* **2011**, *83*, 6913−6917.
(25) Dieringer, J. A.; Lettan, R. B., II; Scheidt, K. A.; Van Duyne, R. P. *J. Am. Chem. Soc.* **2007**, *129*, 16249−16256.
(26) Cao, Y. C.; Jin, R.; Mirkin, C. A. *Science* **2002**, *297*, 1536−1540.

DOI: 10.1021/acs.analchem.7b01267
Anal. Chem. 2017, 89, 8836−8843

(27) Witlicki, E. H.; Andersen, S. S.; Hansen, S. W.; Jeppesen, J. O.; Wong, E. W.; Jensen, L.; Flood, A. H. *J. Am. Chem. Soc.* **2010**, *132*, 6099−6107.
(28) Zhang, L.; Jin, Y.; Mao, H.; Zheng, L.; Zhao, J.; Peng, Y.; Du, S.; Zhang, Z. *Biosens. Bioelectron.* **2014**, *58*, 165−171.
(29) Haiss, W.; Thanh, N. T. K.; Aveyard, J.; Fernig, D. G. *Anal. Chem.* **2007**, *79*, 4215−4221.
(30) Jin, Q.; Shan, L.; Yue, J.; Wang, X. *Food Chem.* **2008**, *108*, 779−783.
(31) Alexander, R. S.; Butler, A. R. *J. Chem. Soc., Perkin Trans. 2* **1976**, 696−701.
(32) Jang, S.; Park, J.; Shin, S.; Yoon, C.; Choi, B. K.; Gong, M. S.; Joo, S. W. *Langmuir* **2004**, *20*, 1922−1927.
(33) Bell, S. E. J.; McCourt, M. R. *Phys. Chem. Chem. Phys.* **2009**, *11*, 7455−7462.
(34) Liu, S. *J. Phys. Chem. A* **2015**, *119*, 3107−3111.
(35) Sheikhian, L.; Bina, S. *J. Chromatogr. B: Anal. Technol. Biomed. Life Sci.* **2016**, *1009-1010*, 34−43.
(36) Absalan, G.; Akhond, M.; Sheikhian, L. *Talanta* **2008**, *77*, 407−411.
(37) Nordstrom, A. C.; Jacobs, F. A.; Eliasson, L. *Plant Physiol.* **1991**, *96*, 856−861.
(38) Wang, P.; Xia, M.; Liang, O.; Sun, K.; Cipriano, A. F.; Schroeder, T.; Liu, H.; Xie, Y. H. *Anal. Chem.* **2015**, *87*, 10255−10261.
(39) Liskova, K.; Kelly, A. L.; O'Brien, N.; Brodkorb, A. *J. Agric. Food Chem.* **2010**, *58*, 4421−4427.
(40) Slaytor, M. B.; Wright, S. E. *J. Med. Pharm. Chem.* **1962**, *5*, 483−491.
(41) Yorgancioglu, A.; Bayramoglu, E. E. *Ind. Crops Prod.* **2013**, *44*, 378−382.

DOI: 10.1021/acs.analchem.7b01267
Anal. Chem. 2017, 89, 8836−8843